J. Heat Treating (1992) 9:91–103

Film and Transition Boiling Correlations for Quenching of Hot Surfaces with Water Sprays

W.P. Klinzing, J.C. Rozzi, and I. Mudawar

Abstract. Using a miniature gold plated copper disk as target, quenching experiments were performed with water sprays to correlate heat flux q'' to surface-to-fluid temperature difference ΔT, and the local values for the spray hydrodynamic parameters of volumetric flux Q'', mean drop velocity U_m and Sauter mean drop diameter d_{32} over a wide range of operating conditions ($Q'' = 0.58 \times 10^{-3}$–$9.96 \times 10^{-3}$ m^3 sec^{-1}/m^2, $U_m = 10.1$–29.9 m/sec, $d_{32} = 0.137$–1.350 mm), and surface temperatures up to 520°C. Drop diameter was found to have a weak effect on heat transfer in film boiling for all the conditions tested. Two distinct spray cooling regimes were identified, allowing the classification of sprays with respect to volumetric flux, low flux sprays for $Q'' < 3.5 \times 10^{-3}$ m^3 sec^{-1}/m^2, and high flux sprays for $Q'' > 3.5 \times 10^{-3}$ m^3 sec^{-1}/m^2. While Q'' had a significant influence on film boiling in both regimes, drop velocity was important only for the high flux sprays. A spray quenching test bed was also constructed to simulate, under controlled laboratory conditions, spray quenching of alloys in an industrial environment. The test bed was used to generate temperature–time records for a rectangular aluminum plate during spray quenching. Using the software package ANSYS, the measured temperature response was successfully simulated by utilizing the newly developed boiling correlations in defining boundary conditions for the quenched surface after accounting for spatial variations in the hydrodynamic parameters within the spray field. The effectiveness of this numerical technique for the tested configuration is proof that it may be possible to predict the temperature–time history for quenched parts with complicated shapes provided the spatial distributions of the hydrodynamic parameters are well mapped or predetermined.

Nomenclature

Bi = Biot number, hw/k_c
C = empirical constant
c_p = specific heat, J/kg·K
d_{32} = Sauter mean diameter (SMD), m
h = convection coefficient, W/m^2·K
h_{fg} = latent heat of vaporization, J/kg
k = thermal conductivity, W/m·K
n_1, n_2, n_3, n_4 = empirical exponents
Nu_{32} = Nusselt number based on Sauter mean diameter, hd_{32}/k_f
Pr = Prandtl number
q'' = heat flux, W/m^2
q''_{CHF} = critical heat flux, W/m^2
Q'' = volumetric flux, m^3 sec^{-1}/m^2
Re_{32} = Reynolds number based on volumetric flux and Sauter mean diameter, $Q'' d_{32}/\nu_f$
t = time, sec
T = temperature, °C
T_{CHF} = temperature corresponding to critical heat flux, °C
T_{DFB} = temperature corresponding to departure from film boiling, °C

The authors are with the Boiling and Two-Phase Flow Laboratory, School of Mechanical Engineering, Purdue University, West Lafayette, IN 47907. Address correspondence to I. Mudawar.

T_{MIN} = temperature corresponding to minimum heat flux, °C
U_m = mean drop velocity, m/sec
w = copper disk thickness, m

Greek Symbols

$\Delta T = T_s - T_f$, °C
$\Delta T_{sat} = T_s - T_{sat}$, °C
$\Delta T_{sub} = T_{sat} - T_f$, °C
ε = emissivity
ν = kinematic viscosity, m^2/sec
ρ = density, kg/m^3
σ = surface tension, N/m; Stefan-Boltzman constant, 5.67×10^{-8} $W/m^2 \cdot K^4$

List of Subscripts

c = copper disk
CHF = critical heat flux
DFB = departure from film boiling
f = liquid
g = vapor
MIN = minimum heat flux
s = surface
sat = saturation
sub = subcooled
∞ = ambient

Introduction

Processing of alloys by extrusion, forging, or casting with any degree of control over the metallurgical and mechanical properties demands careful control of heat removal from the product. The rate of heat removal during the cooling that follows the forming process has a significant influence on hardness, strength, and the occurrence of residual stresses, often resulting in stress concentration or cracking. In many of the metal forming processes, the product is cooled by water sprays after exiting a die, a procedure commonly referred to as press quenching. It is common practice for the operator to configure the sprays (i.e., set the nozzle position and flow rate) based upon prior experience, and later perturb the sprays by trial and error until a configuration is found which most closely approaches meeting the desired product specifications. After the press quenching, a costly posttreatment, consisting of additional heat treating and cold working, may be necessary to meet these specifications. This posttreatment is often the result of poor control over the quenching process, and may result in a large cost penalty for the metal forming operation and consumer.

The objective of the spray quenching research program at the Purdue University Boiling and Two-Phase Flow Laboratory since 1985 has been to provide the knowledge and means to predict the proper configuration of sprays to virtually eliminate the need for posttreatment. This has been proposed by generating extensive heat transfer and materials data bases, and integrating these data bases using a generic CAD methodology which can easily be applied to different types of spray nozzles and a multitude of materials. In implementing this semiexpert technology the operator would simply enter into the computer the product geometry and desired material properties, and the CAD system would then consult and integrate its data bases and output a number of acceptable spray configurations. Complexity and stringent product specifications may necessitate automating the positioning of the nozzles and the throttling of spray flow rate using sensors and motorized translation platforms, both of which can also be directly interfaced with, and controlled by the CAD system.

A key guide to understanding the cooling performance of sprays is the relationship between heat flux from the quenched surface and surface temperature—the boiling curve. At any given surface temperature, a larger heat flux amounts to a faster rate of cooling for the surface. The relationship between heat flux and surface temperature undergoes drastic changes during the quench, triggered by changes in the mechanism of water contact with the surface between the various regions of the boiling curve. Figure 1 shows a boiling curve associated with quenching of a metallic product in a stagnant bath of liquid. For most quenching operations the product surface is cooled from an initial high temperature usually well in excess of the point of departure from film boiling (DFB; point E in Fig. 1). During the initial moments of the quench the surface experiences what is known as film boiling, where a continuous vapor layer (blanket) forms on the surface preventing the water from making direct contact with the surface. A slight collapse in the vapor blanket at point E causes some enhancement in heat flux. This weak enhancement persists down to the minimum heat flux point (MIN; point D in Fig. 1), where collapse of the vapor layer promotes appreciable wetting of the surface, a transition marked by a significant increase in the heat flux causing a rapid decrease in surface temperature. The region between points D and C is called transition boiling, where parts of the surface undergo wetting (and vigorous boiling) with liquid, while others remain in film boiling. Point C is the critical heat flux point below which (down to point A) the entire

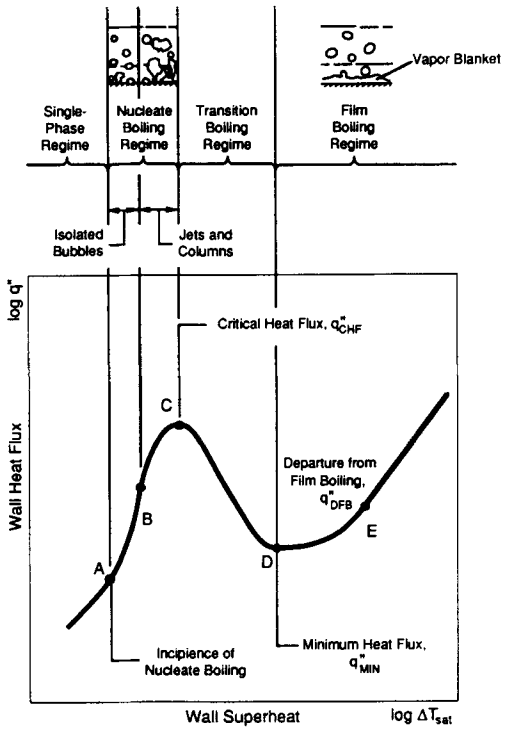

Fig. 1. Boiling curve for a hot surface in a stagnant pool of liquid at its saturation temperature.

surface becomes available for nucleate boiling. Below point A boiling completely subsides and direct heat transfer to the liquid follows without evaporation.

Spray quenching involves transition between the various boiling regions indicated in Figure 1, occurring within drops as they impact the surface individually or coalesce with other drops or both. Complications incurred in determining the exact heat flux–surface temperature relationship include effects such as those of surface roughness and the hydrodynamic structure of the spray. Combined, these effects can cause the temperature corresponding to minimum heat flux to vary from 300 to as high as 900°C [1]. In almost all of the literature reviewed by the authors, the relevant hydrodynamic parameters necessary to characterize spray heat transfer were volumetric flux (i.e., water flow rate per unit surface area) [2–7], drop velocity [3,5–8] and drop diameter [6–8].

Some investigators [5–7], because of differences in the relative importance of parameters governing spray heat transfer in film boiling, found it necessary to classify water sprays into two regimes, that of dilute (low volumetric flux) sprays and dense (high volumetric flux) sprays. While volumetric flux was found to be the trenchant parameter for both regimes, other parameters such as drop diameter, drop velocity, and Weber number were found to influence heat transfer in the case of dilute sprays.

During the quenching process, an abrupt increase in the heat flux occurs following the departure from film to transition boiling. The temperature at which this departure takes place is sometimes referred to as the Leidenfrost temperature (there is some confusion in the literature on whether the Leidenfrost temperature coincides with points E or D in Figure 1). Due to the sparse nature of work related to the Leidenfrost temperature for water sprays, it is difficult to draw any definitive conclusions concerning the physical mechanisms governing the Leidenfrost phenomenon. However, from the limited information available, it appears that volumetric flux is again the most influential parameter affecting the Leidenfrost temperature [1,9]. Also, experiments performed with single droplets seem to be of little or no value in characterizing the Leidenfrost temperature for sprays [1].

While heat transfer correlations for the film boiling region and the minimum heat flux point are of great importance in most metal forming processes, quenching of aluminum parts can be sensitive to lower temperature regions of the boiling curve as well (i.e., transition and nucleate boiling). Recently, Mudawar and Valentine [10] developed heat transfer correlations for the transition, nucleate, and single-phase regions using an electrically heated calorimeter bar exposed at one end to the spray. Their correlations were presented as functions of the local hydrodynamic parameters of the spray (volumetric flux, drop diameter and drop velocity). Unfortunately, temperature limitations imposed by their calorimeter bar design precluded testing in the film boiling region and made it difficult to obtain measurement in the transition boiling region, except for a few dilute sprays.

Deiters and Mudawar [11] investigated the spatial distributions of the spray hydrodynamic parameters and the effect of these distributions on cooling rate. Using measured as well as mathematically fitted hydrodynamic distributions, they demonstrated that the correlations developed by Mudawar and Valentine were spatially independent and applicable to all types of sprays (e.g., full cone, hollow cone, flat) employed in materials processing.

This paper presents new correlations for film boiling, point of departure from film boiling, point of minimum heat flux and transition boiling, providing knowledge which compliments the study by Mudawar and Valentine in characterizing the various regions of the boiling curve for water sprays. Also presented is the description of a spray quenching test

bed which was constructed for simulating, under controlled laboratory conditions, spray quenching of alloys in an industrial environment. Validity of the correlations developed for each regime is examined by comparing numerical predictions with ANSYS to the temperature response of an aluminum plate measured during quenching in the test bed.

Experimental Methods

In order to develop and then assess the validity of the spray quenching correlations, two experimental facilities were utilized. First an extensive data base was collected using a single spray quench facility, the details of which can be found elsewhere [10]. From this data base the correlations were developed. These correlations were then examined for the case of a series 1100-0 aluminum plate using the newly constructed spray quenching test bed. Measurements obtained in the test bed served as test cases for numerical modeling using the software package ANSYS. The description of the two facilities follows.

Single Spray Quench Chamber

The film and transition boiling correlations were developed from quench data measured at the geometric center of the spray inside the spray chamber illustrated in Figure 2. This is the same chamber utilized by Mudawar and Valentine in their earlier spray work. Embedded in an insulating casing at the spray center was the quench target, a 7.94 mm diameter oxygen-free copper disk with a thickness of 3.56 mm. Temperature was measured by a Chromel-Alumel thermocouple made from 0.127 mm wire, which was spot welded to the disk underside. The disk was gold plated to enhance resistance to oxidation at the high temperatures associated with film boiling. Previous studies have shown traces of oxidation on copper during prolonged quenching even at temperatures within the transition boiling region [10].

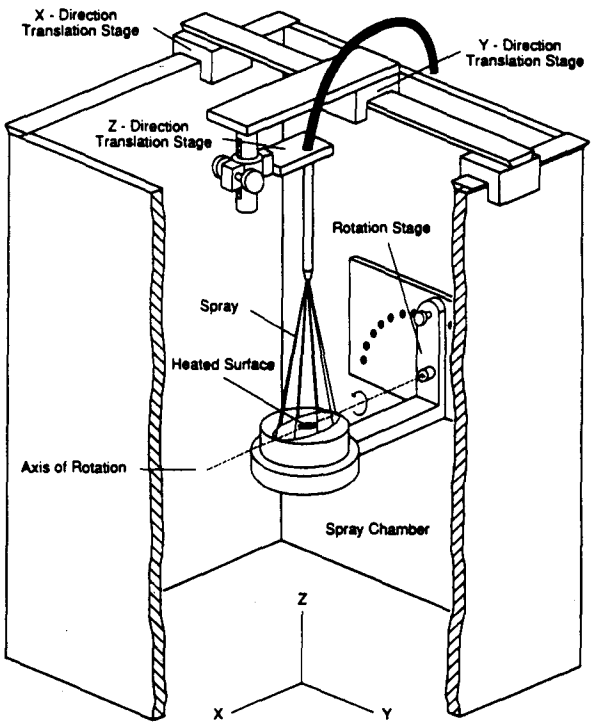

Fig. 2. Cross-sectional view of spray chamber in the single spray facility.

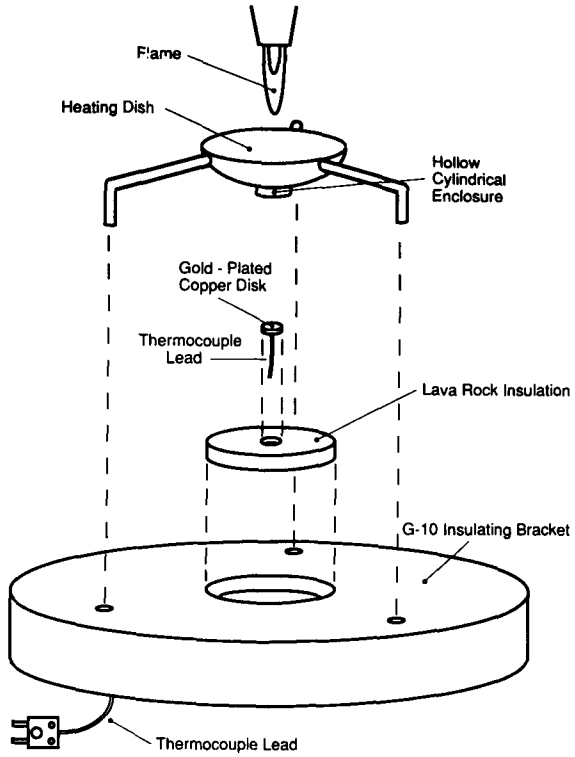

Fig. 3. Schematic of copper disk assembly.

The gold plated copper disk was designed to maintain a ratio of thermal resistance due to conduction within the disk to the resistance due to convection at the quench surface—the Biot number (Bi)—well below 0.1. This allowed the heat transfer coefficient to be determined experimentally by solving the inverse heat diffusion equation assuming lumped capacitance in the disk.

As shown in Figure 3, the copper disk was preheated to an initial temperature of approximately 530°C using an oxyacetylene torch. The flame was directed against a heat shield which prevented the gold plate on the disk surface from melting. The

pump was then engaged and the spray, which was prevented from contacting the target by a diversion device, was allowed to reach hydrodynamic equilibrium (purging of air from the water supply line caused occasional pulsation of flow during start-up). The torch and the diversion device were then quickly removed permitting commencement of the quench. Temperature was recorded every 20 msec during the quench and written to a data file for later processing.

Spray Quenching Test Bed

The test bed consisted of a preheating furnace, translation platform for the testpiece, spray chamber, water reservoir, and external plumbing as shown in Figure 4. These components (excluding the plumbing) were supported by a carbon steel frame which measured 1.35 × 1.35 × 2.69 m high. Including the furnace, the overall height of the system measured 3.91 m. The entire frame rested on a single welded platform to the bottom of which lifter pads were welded to ensure an even distribution of the system weight.

The testpiece was heated to a uniform temperature in a vertically oriented tube furnace having three independently controlled heating zones which ensured uniform heating over 70 cm of the furnace length. A Maulite process tube was installed coaxially inside the furnace to shield the testpiece against contact with the furnace heating elements as shown in Figure 5. To avoid exerting any load on the fragile refractory brick inside the furnace, the process tube was supported by three posts which were affixed to a plate bolted to the sturdy steel frame external to the furnace. A three-zone programmable controller was used to monitor and manipulate furnace heat up rates.

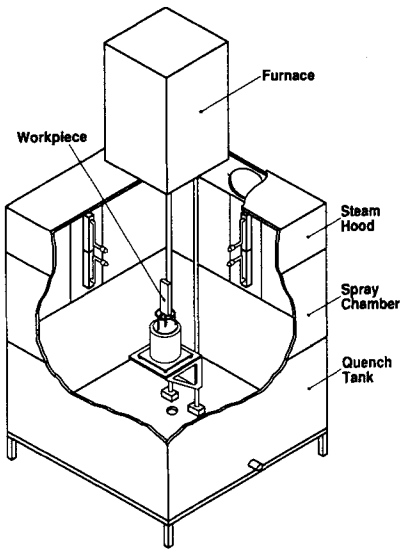

Fig. 4. Cutaway view of spray quenching test bed.

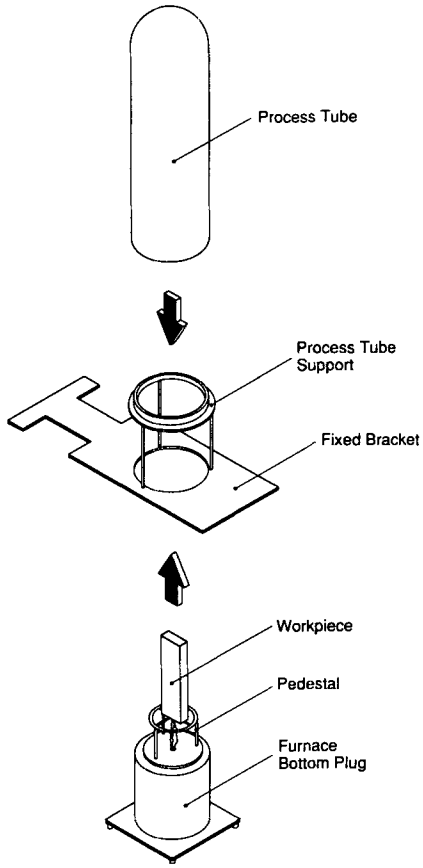

Fig. 5. Schematic of testpiece and process tube support assembly.

The testpiece was transported from the furnace to the spray chamber on a translation platform with the aid of a counterweight. The translation platform rode on two stainless steel shafts which were held in position by shaft mounts placed at the bottom of the quench tank and on the process tube support plate located directly beneath the furnace. These mounts also allowed for thermal expansion of the shafts to prevent buckling during workpiece descent. Mounts on one of the shafts were equipped with aluminum sliding mechanisms which made adjustable the distance between the shafts and minimized shaft skew.

Water stored in the tank at the bottom of the test bed passed through a strainer before entering a centrifugal pump rated to deliver 25.2 × 10^{-3} m^3/sec (40 gal/min) at 689 kPa (100 psi) and temperatures up to 82°C. Due to the large capacity of the pump, most of the flow was bypassed to the tank via a regulating globe valve. The spray water continued

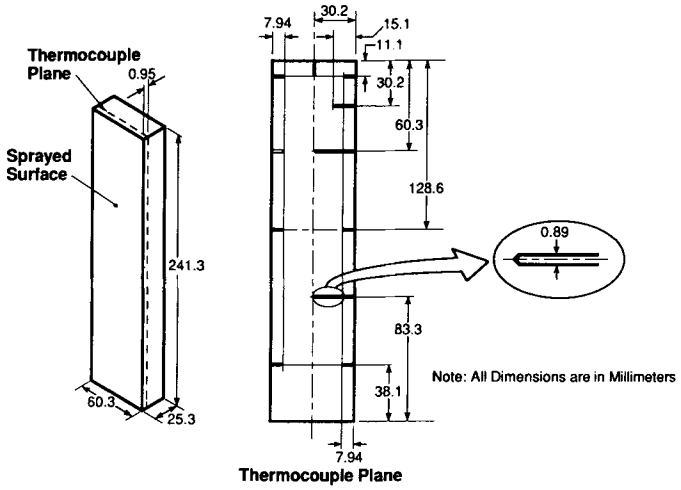

Fig. 6. Construction of the aluminum testpiece.

through a 5 μm filter followed by a heat exchanger before being directed into eight supply lines, each fitted with a globe valve followed by a pressure gage and a heavy duty rubber hose leading to the spray nozzle. Following impingement onto the testpiece, liquid supplied through each spray nozzle was collected in the reservoir for recirculation. The frame of the spray chamber itself was fitted within the large frame supporting the test bed hardware. One aluminum plate was located along the center of each of the four sides of the spray chamber providing support for the nozzle plumbing, with all the remaining surfaces of the spray chamber covered with transparent polycarbonate plastic. Nozzle mounts connected to the aluminum plates featured flexibility in the positioning of the nozzles at any desired location relative to the testpiece.

Figure 6 shows details of the instrumented workpiece used to assess the validity of the newly developed correlations for large surfaces. It consisted of a series 1100-0, 2.52 cm thick aluminum plate having a quench area of 24.13 × 6.03 cm which was blasted with silica particles to ensure uniform surface finish having a characteristic cavity size of 10 μm. The plate was instrumented with 11 thermocouples positioned in a plane 0.508 mm away from the quench surface. The thermocouples were constructed from 0.127 mm Chromel-Alumel (type K) wire set in a 0.813 mm Inconel sheath and insulated with magnesium oxide. Boron nitride powder filled the gap between the thermocouple bead and the aluminum, enhancing thermal contact and thermocouple temperature response.

The aluminum bar was raised into the furnace by pulling the counterweight of the translation platform, and then heated well into the film boiling region. Once the desired starting temperature (550 to 555°C) was reached, the pump was engaged and the sprays allowed to come to hydrodynamic equilibrium. The testpiece was then quickly lowered into the spray chamber and the temperature response of selected thermocouples recorded with a maximum sampling rate of 50 msec.

Development of the Correlations

As indicated in the Introduction, most investigators have correlated film boiling heat transfer data for sprays with respect to surface-to-fluid temperature difference ΔT $(= T - T_f)$, and volumetric flux Q''. Although some have reported secondary effects due to drop velocity and drop diameter, conclusions concerning these effects are often highly uncertain and this uncertainty is primarily the result of limitations on the ranges of drop velocity and drop diameter attainable from commercial sprays. It is for this reason that efforts were made in the present study to select nozzles which provided fairly extensive ranges for each of the hydrodynamic parameters, allowing in several cases for variation in one parameter while holding the other two constant.

One flat spray nozzle and four different full-cone nozzles were used in 26 tests to provide the following ranges of hydrodynamic parameters: $Q'' = 0.58 \times 10^{-3}$–$9.96 \times 10^{-3}$ $m^3\,sec^{-1}/m^2$, $U_m = 10.1$–29.9 m/sec and $d_{32} = 0.137$–1.350 mm. Variation in the hydrodynamic parameters for the same nozzle was achieved by changing nozzle-to-surface distance and/or supply pressure. For each of the tests, the temperature–time history was recorded and later processed to determine the relationship between heat flux, q'', and wall temperature difference, ΔT.

Using the lumped capacitance method, temperature throughout the 3.56 mm thick copper disk was assumed to be uniform at every instant during the quench. Therefore, the surface temperature and temperature recorded by the thermocouple spot welded to the disk underside were assumed equal. To further reduce error in using the lumped capacitance method, data was only used which corresponded to $Bi < 0.05$ ($h < 5149$ W/m^{2}K). Data corresponding to Bi exceeding this value during the later stages of the quench (i.e., part of the transition boiling region and all of the nucleate boiling and single-phase regions) were discarded.

From the measured temperature response, a derivative for each time increment was computed from a centered, second order, 11 point least squares fit to the data (i.e., the derivative was calculated at the sixth point in each 11 point fit), and from the derivative the heat flux was determined from the equation

$$q'' = -\rho_c c_{p,c} w \frac{dT}{dt}. \quad (1)$$

where ρ_c, $c_{p,c}$ and w are the density, specific heat, and thickness of the copper disk, respectively. Figure 7 shows an example of temperature–time plots generated for the copper disk for increasing volumetric flux. The corresponding quench curves displayed in Figure 8 were determined using the lumped capacitance method.

Figure 8 clearly demonstrates that the slope of the heat flux versus temperature drop curve is lower for spray fluxes exceeding approximately 3.5×10^{-3} m^3 sec^{-1}/m^2 than for lower spray fluxes. The data base was, therefore, divided into two ranges: low spray flux for $Q'' < 3.5 \times 10^{-3}$ m^3 sec^{-1}/m^2 and high spray

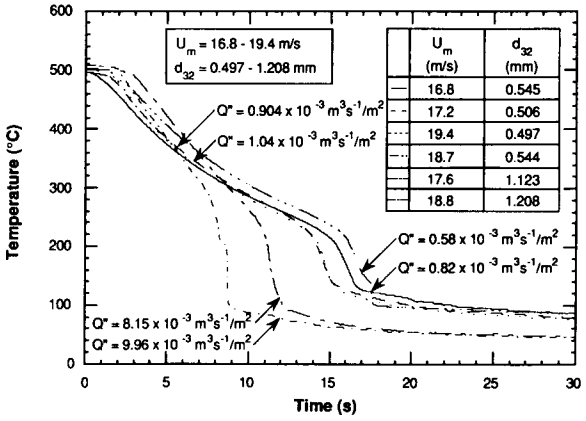

Fig. 7. Variation of temperature response of the copper disk with increasing volumetric flux.

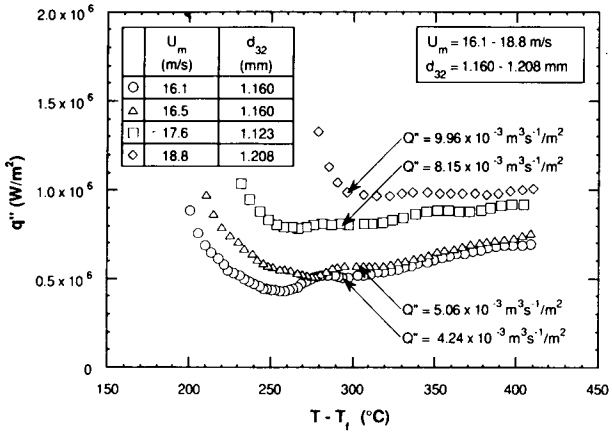

Fig. 8. Variation of the copper disk boiling curve with increasing volumetric flux.

flux for $Q'' > 3.5 \times 10^{-3}$ m^3 sec^{-1}/m^2. Assuming heat flux correlations of the form

$$q'' = C\Delta T^{n_1} Q''^{n_2} U_m^{n_3} d_{32}^{n_4} \quad (2)$$

the ΔT exponent was determined by averaging exponents for all the tests in each volumetric flux range, which resulted in the values 1.691 and 0.461 for the low flux and high flux ranges, respectively. In determining the exponents in the high flux range, exponents for the individual tests were weighted to ensure equal representation of data over the range 4×10^{-3}–9×10^{-3} m^3 sec^{-1}/m^2 since more tests were concentrated toward 4×10^{-3} m^3 sec^{-1}/m^2 in the high flux range. With the exponent of ΔT known, correlation of the film boiling heat flux to the hydrodynamic parameters was accomplished by a least squares fit to the data, resulting in the following film boiling correlations:

Low spray flux ($0.58 \times 10^{-3} < Q'' < 3.5 \times 10^{-3}$ m^3 sec^{-1}/m^2):

$$Q'' < 3.5 \times 10^{-3} \text{ m}^3 \text{ sec}^{-1}/\text{m}^2: \quad q'' = 63.250\, \Delta T^{1.691} Q''^{0.264} d_{32}^{-0.062} \quad (3)$$

High spray flux ($9.96 \times 10^{-3} > Q'' > 3.5 \times 10^{-3}$ m^3 sec^{-1}/m^2):

$$Q'' > 3.5 \times 10^{-3} \text{ m}^3 \text{ sec}^{-1}/\text{m}^2: \quad q'' = 141345\, \Delta T^{0.461} Q''^{0.566} U_m^{0.639} \quad (4)$$

Figures 9(a) and (b) show the film boiling correlations plotted against the respective data in each range and the associated mean absolute error and maximum error. Equations (3) and (4) demonstrate

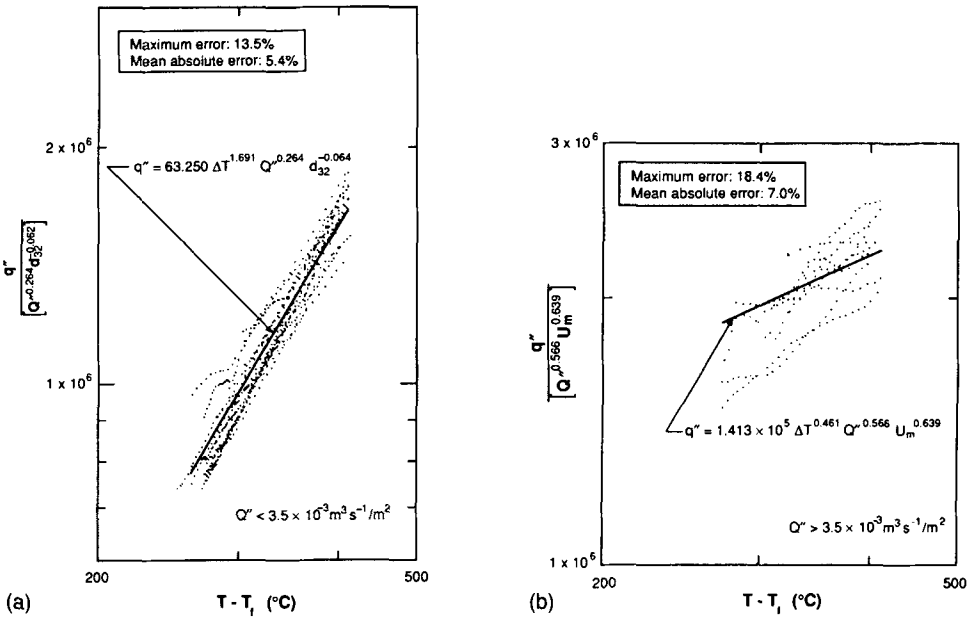

Fig. 9. Correlation of film boiling for (a) low volumetric spray flux and (b) high volumetric spray flux.

that drop diameter has a negligible effect on film boiling heat flux for the conditions investigated. While volumetric flux is shown to have an important effect on heat flux in both ranges, mean drop velocity seems to play a paramount role in spray heat transfer in the high spray range and none in the low flux one.

The technique described above was also employed to develop correlations for the points on the quench curve corresponding to departure from film boiling and minimum heat flux

Low flux:

$$q''_{\mathrm{DFB}} = 6.100 \times 10^6\, Q''^{0.588} U_m^{0.244} \tag{5}$$

$$\Delta T_{\mathrm{DFB}} = 2.808 \times 10^2\, Q''^{0.087} U_m^{0.110} d_{32}^{-0.035} \tag{6}$$

$$q''_{\mathrm{MIN}} = 3.324 \times 10^6\, Q''^{0.544} U_m^{0.324} \tag{7}$$

$$\Delta T_{\mathrm{MIN}} = 2.049 \times 10^2\, Q''^{0.066} U_m^{0.138} d_{32}^{-0.035} \tag{8}$$

High flux:

$$q''_{\mathrm{DFB}} = 6.536 \times 10^6\, Q''^{0.995} U_m^{0.924} \tag{9}$$

$$\Delta T_{\mathrm{DFB}} = 3.079 \times 10^4\, Q''^{-0.194} U_m^{1.922} d_{32}^{1.651} \tag{10}$$

$$q''_{\mathrm{MIN}} = 6.069 \times 10^6\, Q''^{0.943} U_m^{0.864} \tag{11}$$

$$\Delta T_{\mathrm{MIN}} = 7.990 \times 10^3\, Q''^{-0.027} U_m^{1.033} d_{32}^{0.952} \tag{12}$$

Errors associated with each of the above correlations are given in Table 1.

Numerical Simulation

Coupled with heat transfer correlations recently developed at Purdue's Boiling and Two-Phase Flow Laboratory for the other boiling regimes [10], the correlations of the present study were utilized as boundary conditions in a numerical simulation of quenching of the aluminum plate shown in Figure 6 using the software package ANSYS. The numerical predictions are compared to quench curves for various points in the aluminum plate measured experimentally in the test bed. A compilation of all the correlations utilized in the numerical simulation is presented in Table 2.

Problem solving using ANSYS is comprised of three distinct phases: preprocessing, solution, and postprocessing. Preprocessing involves the development of all the information necessary for the solution phase, such as generating the solid model and specifying the material properties and boundary conditions. The solution phase is executed internal to the software and is not accessible to the user. The postprocessing phase is where the user may display or write to files variables of his choosing.

Experimentally, two flat sprays, one positioned vertically above the other, provided a fairly complete coverage of the sprayed surface of the aluminum plate, creating a nearly two-dimensional boundary condition. Using the spatial distributions for the hydrodynamic parameters measured by Deiters and Mudawar [11] for the same spray conditions used in

Table 1. Errors Associated with the Correlation of Heat Flux and Wall Temperature Drop for the Points of Departure From Film Boiling and Minumum Heat Flux in each Spray Flux Range

	Maximum Error				Mean Absolute Error			
	q''_{DFB} (W/m²)	ΔT_{DFB} (°C)	q''_{MIN} (W/m²)	ΔT_{MIN} (°C)	q''_{DFB} (W/m²)	ΔT_{DFB} (°C)	q''_{MIN} (W/m²)	ΔT_{MIN} (°C)
High Q'' range	11.2%	0.9%	12.0%	4.9%	8.1%	0.4%	7.8%	2.4%
Low Q'' range	17.3%	9.1%	20.5%	9.6%	7.1%	2.6%	9.0%	3.1%

Table 2. Summary of Spray Heat Transfer Correlations

Boiling (Quenching) Region	Correlation
Film boiling	$Q'' > 3.5 \times 10^{-3}$: $q'' = 1.413 \times 10^5 \Delta T^{0.461} Q''^{0.566} U_m^{0.639}$
	$Q'' < 3.5 \times 10^{-3}$: $q'' = 63.250 \Delta T^{1.691} Q''^{0.264} d_{32}^{-0.062}$
Point of departure from film boiling	$Q'' > 3.5 \times 10^{-3}$: $q''_{DFB} = 65.361 \times 10^5 Q''^{0.995} U_m^{0.924}$
	$\Delta T_{DFB} = 30793.201 Q''^{-0.194} U_m^{1.922} d_{32}^{1.651}$
	$Q'' < 3.5 \times 10^{-3}$: $q''_{DFB} = 61.003 \times 10^5 Q''^{0.588} U_m^{0.244}$
	$\Delta T_{DFB} = 280.762 Q''^{0.087} U_m^{0.110} d_{32}^{-0.035}$
Film wetting region	$q'' = N_0 + N_1 \Delta T + N_2 \Delta T^2$
	$N_0 = q''_{MIN} - N_1 \Delta T_{MIN} - N_2 \Delta T_{MIN}^2$
	$N_1 = -2 N_2 \Delta T_{MIN}$
	$N_2 = \frac{q''_{DFB} - q''_{MIN}}{(\Delta T_{DFB} - \Delta T_{MIN})^2}$
Minimum heat flux point	$Q'' > 3.5 \times 10^{-3}$: $q''_{MIN} = 60.694 \times 10^5 Q''^{0.943} U_m^{0.864}$
	$\Delta T_{MIN} = 7990.273 Q''^{-0.027} U_m^{1.330} d_{32}^{0.952}$
	$Q'' < 3.5 \times 10^{-3}$: $q''_{MIN} = 33.244 \times 10^5 Q''^{0.544} U_m^{0.324}$
	$\Delta T_{MIN} = 204.895 Q''^{0.066} U_m^{0.138} d_{32}^{-0.035}$
Transition boiling	$q'' = q''_{CHF} - \frac{q''_{CHF} - q''_{MIN}}{(\Delta T_{CHF} - \Delta T_{MIN})^3} [\Delta T_{CHF}^3 - 3\Delta T_{CHF}^2 \Delta T_{MIN} + 6\Delta T_{CHF} \Delta T_{MIN} \Delta T - 3(\Delta T_{CHF} + \Delta T_{MIN}) \Delta T^2 + 2\Delta T^3]$
Critical heat flux [10]	$\frac{q''_{CHF}}{\rho_g h_{fg} Q''} = 122.4 \left[1 + 0.0118 \left(\frac{\rho_f}{\rho_g}\right)^{1/4} \left(\frac{\rho_f c_{p,f} \Delta T_{sub}}{\rho_g h_{fg}}\right)\right] \left(\frac{\sigma}{\rho_f Q''^2 d_{32}}\right)^{0.198}$
	$\Delta T_{CHF} = 18 \left[(\rho_g h_{fg} Q'') \left(\frac{\sigma}{\rho_f Q''^2 d_{32}}\right)^{0.198}\right]^{1/5.55}$
Nucleate boiling [10]	$q'' = 1.87 \times 10^{-5} (\Delta T)^{5.55}$
Incipient boiling [10]	$\Delta T = 13.43 Re_{32}^{0.167} Pr_f^{0.123} \left(\frac{k_f}{d_{32}}\right)^{0.220}$
Single phase cooling [10]	$Nu_{32} = 2.512 Re_{32}^{0.167} Pr_f^{0.56}$

NOTES: Units of the parameters are: q''(W/m²), ΔT(°C), Q''(m³ sec⁻¹/m²), U_m(m/sec), d_{32}(m), ρ_f(kg/m³), ρ_g(kg/m³), $c_{p,f}$(J/kg K), h_{fg}(J/kg), σ(N/m).

Ranges of validity of the correlations are: $Q'' = 0.6\text{–}9.96 \times 10^{-3}$ m³ sec⁻¹/m², $U_m = 10.1\text{–}26.7$ m/sec and $d_{32} = 405 \times 10^{-3}\text{–}1350 \times 10^{-3}$ m, $T_f = 23$°C.

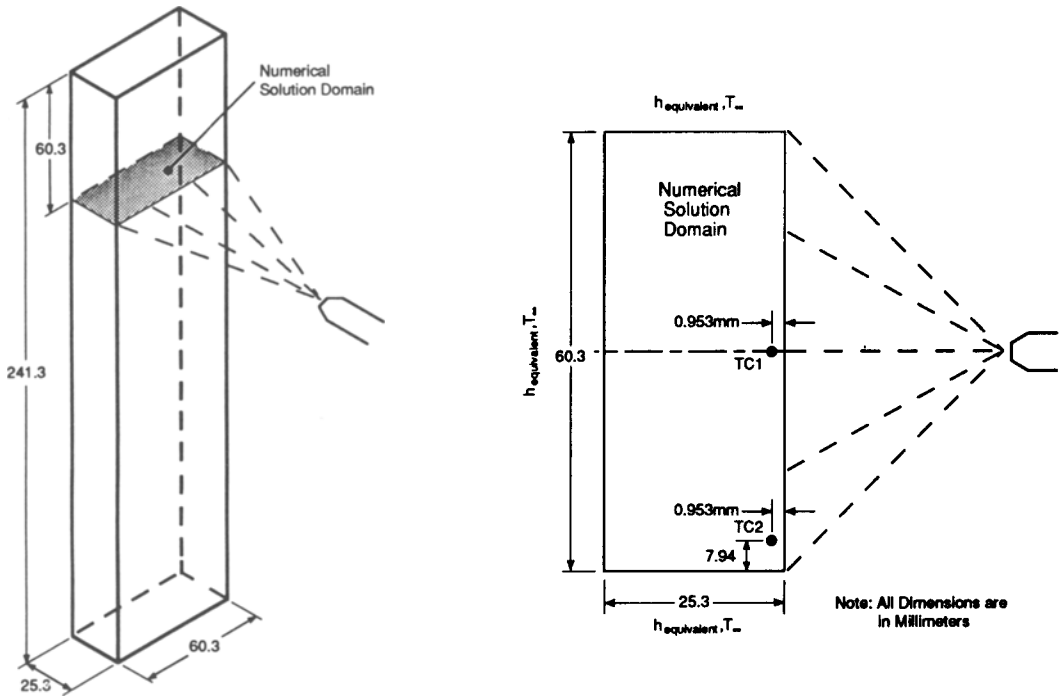

Fig. 10. Location of numerical solution domain and thermocouples TC1 and TC2 with respect to the aluminum plate.

the present study, local values for Q'', d_{32}, and U_m were calculated along the minor axis of the spray for the numerical domain shown in Figure 10. The computed values for the local hydrodynamic parameters, Figure 11, were then used in the correlations given in Table 2 to determine the heat transfer boundary conditions for the sprayed surface.

Radiative and convective losses from the unsprayed surfaces were accounted for through an equivalent heat transfer coefficient defined as:

$$h_{\text{equivalent}} = h_{\text{convection}} + h_{\text{radiation}} \tag{13}$$

where

$$h_{\text{radiation}} = \varepsilon\sigma(T_s + T_\infty)(T_s^2 + T_\infty^2) \tag{14}$$

Losses due to natural convection were computed using an average heat transfer coefficient for a vertical height equal to that of the plate computed from a correlation by Churchill and Chu (see ref. [12]). Values estimated for $h_{\text{equivalent}}$ ($\approx$28 W/m^{2}K) were negligible compared to the heat transfer coefficient of film boiling on the sprayed surface.

ANSYS was used to predict the temperature response for points corresponding to thermocouples T1 and T2 located as shown in Figure 10, and a comparison of the predicted to the measured response is shown in Figure 12(a) and (b). Thermocouple T1 was positioned along the geometric center of the spray field, where all the spray heat transfer correlations given in Table 2 were developed, and T2 was located closer to the outer edge of the spray field. Fair agreement was achieved in both cases and with a similar degree of accuracy, confirming a conclusion arrived at earlier by Deiters and Mudawar [11] for a quench initiated in transition boiling, that heat transfer correlations developed for the center are valid for other points in the spray field, provided these correlations are based upon the local values of the hydrodynamic parameters.

Several reasons exist for the discrepancies between the ANSYS predictions and experimental data. The most obvious is that the two-dimensional numerical solution does not properly account for heat diffusion perpendicular to the solution domain. The actual field of each of the two sprays (which were positioned one vertically above the other to quench one surface of the aluminum plate) takes the form of an ellipse with a large ratio of major to minor axis. This feature of the flat sprays promoted a rather two-dimensional cooling pattern on the sprayed surface. Nevertheless, the numerical solution domain coincides with the quenched surface along the minor axis of the upper spray, a region of slightly higher volumetric flux (i.e., higher heat transfer coefficient) than the rest of the spray field; consequently, as heat was being extracted by the spray from this region, some

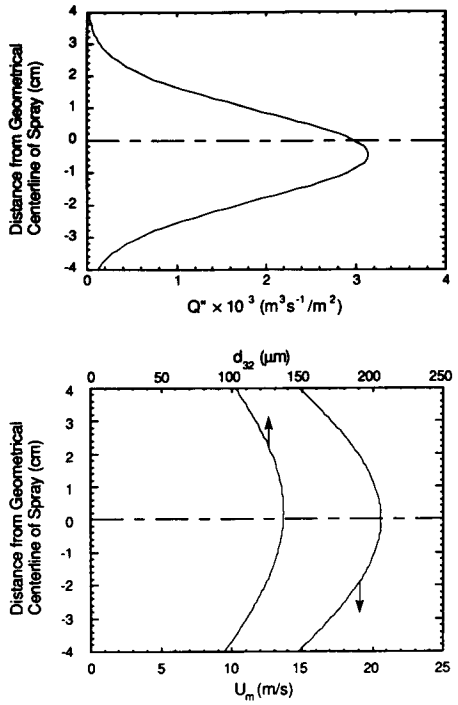

Fig. 11. Two-dimensional curve fits to spatial distributions of Q'', U_m and d_{32} measured by Deiters and Mudawar along the minor axis of the flat spray.

heat was also being imported from regions in the plate located above and below the numerical solution domain where heat flux to the water spray was relatively low. Since the numerical model is two dimensional it could not account for this heat addition and therefore slightly overpredicted the cooling rate.

Also contributing to error in the numerical predictions are the approximations in determining the spatial distributions of the hydrodynamic parameters themselves. The distributions for the two flat sprays used in the present study were approximated by distribution functions of a similar spray nozzle measured by Deiters and Mudawar. Machining tolerances are known to alter the hydrodynamic characteristics for nozzles of identical part number and this can cause differences in cooling performance between the two nozzles used in the present study as well as between each and the nozzle used by Deiters and Mudawar.

Small deviations in the single-phase region of the boiling curve evident from Figure 12(a) and (b) can be the result of liquid run-off along the sprayed surface due to the lack of vaporization of liquid upon impacting the surface. Under the influence of gravity, the vertical orientation of the plate may cause water impacting the top portion to fall down the plate, heating up as it traverses its length. This heated liquid can impair the effectiveness of droplet impact

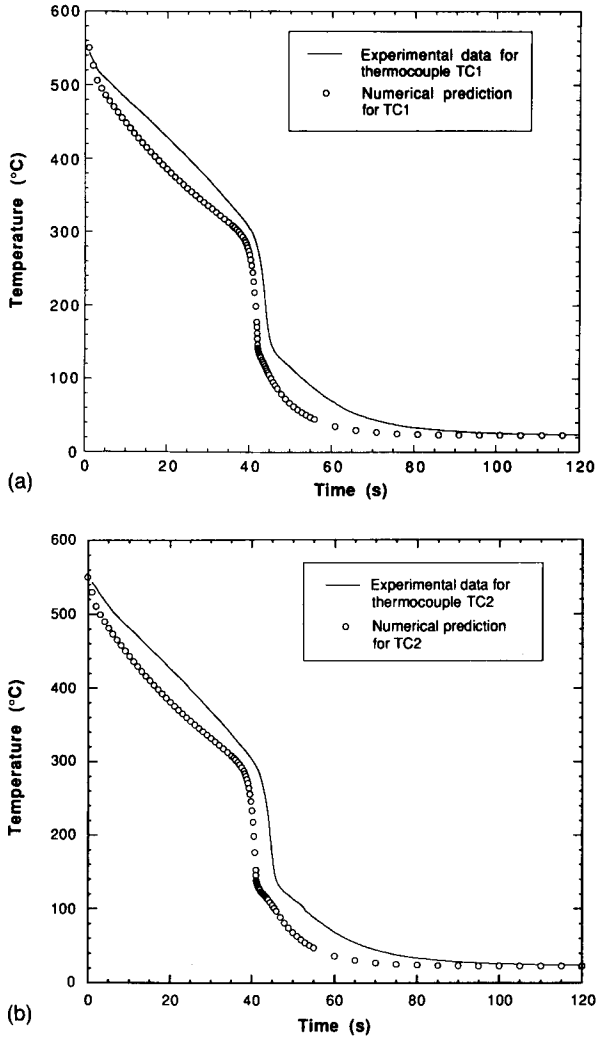

Fig. 12. ANSYS predicted temperature response for points corresponding to (a) thermocouple TC1 and (b) thermocouple TC2.

with the sprayed surface, thereby influencing local spray heat flux. It is very important to note, however, that the numerical predictions are important to materials processing only in the film, transition, and nucleate boiling regions, which are most responsible for determining the metallurgical properties of the alloy.

Figure 13 shows the numerically predicted temperature distributions for the solution domain for times corresponding to the center of the sprayed undergoing film boiling, transition boiling, nucleate boiling, and single-phase cooling, respectively. These distributions demonstrate the strong effect of volumetric flux on heat flux in the various regions of the boiling curve. At the onset of the numerically simulated quench, the higher volumetric fluxes toward

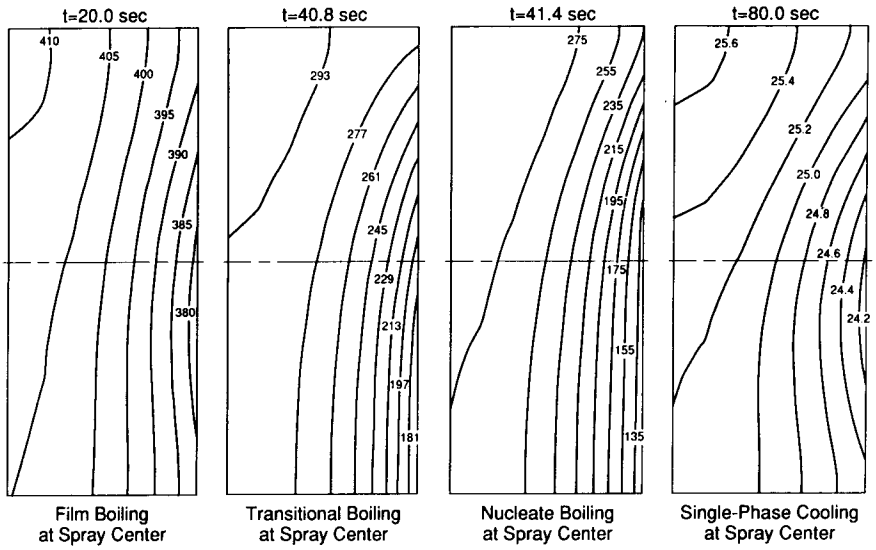

Fig. 13. ANSYS predicted temperature for selected times during the quench.

the center of the spray promote faster cooling near the center and a delayed response to the quench toward the corners. As indicated earlier, the distribution functions for the hydrodynamic parameters used in determining the heat transfer boundary conditions for the sprayed surface were distorted slightly away from the geometrical center of the spray according to the measurements of Deiters and Mudawar, which were also adopted in the present numerical simulation, due to minute imperfections in the manufacturing of spray nozzles. The small displacement of the point of maximum volumetric flux from the geometrical center produced a similar displacement of the coolest surface point slightly away from the center as shown in Figure 13 for t = 20 sec. It is important to note that, despite their small magnitude during film boiling, surface temperature distortions can lead to pronounced distortions in the transition and nucleate boiling regions as shown in Figure 13 for t = 40.8 and 41.4 sec. Asymmetry in surface temperature during film boiling seems to promote wetting on one side of the spray center earlier than on the other side. The sudden drastic increase in heat flux immediately following wetting renders the wetting side very favorable for heat to be transferred from the aluminum plate, resulting in an even greater asymmetry in the temperature distribution.

The numerical findings of the present study demonstrate the importance of carefully mapping the spatial distributions of the hydrodynamic parameters in order to numerically simulate temperature response with any reasonable accuracy. Conversely, the results point to a need for spray nozzles manufactured with much closer tolerances if any predictability and/or repeatability are to be realized in the quenching process. As indicated earlier in this paper, the ultimate goal in a controlled spray quenching environment is to optimize the spray configuration in order to achieve temperature response within a narrow window, prescribed by a minimum, corresponding to the need to produce the desired material properties, and a maximum, above which large temperature gradients in the quenched part may lead to unacceptable stress concentration causing warping or cracking of the part. This goal becomes very challenging with complex shapes as section thickness varies in different regions of the quenched part and/or varying material properties are to be developed for different regions. These challenges are further evidence of the need for spray nozzles with predictable and repeatable performance.

Acknowledgments. Financial support for this work by the Purdue University Engineering Research Center for Intelligent Manufacturing Systems is gratefully appreciated. The authors thank Messrs. Jerry Hagers and Rudolf Schick of Spraying Systems Co., and Gerry Dail of ALCOA for their valuable technical assistance.

References

1. C.J. Hoogendoorn and R.d. Hond, "Leidenfrost Temperature and Heat-Transfer Coefficients for Water Sprays Impinging on a Hot Surface," Proc. 5th International Heat Transfer Conference, 1974, pp. 135–138.
2. E.A. Mizikar, "Spray Cooling Investigation for Continuous Casting of Billets and Blooms," *Iron and Steel Engineering*, 1970, Vol. 47, pp. 53–60.

3. H. Muller and R. Jeschar, "Untersuchung des Warmeubergangs an einer Simulierten Sekundarkuhlzone beim Stranggiebverfahren," *Arch. Eisenhuttenwes*, 1973, Vol. 44, pp. 589–594.
4. L.I. Urbanovich, V.A. Goryainov, V.V. Sevost-'yanov, Y.G. Boev, V.M. Niskovskikh, A.V. Grachev, A.V. Sevost'yanov, and V.S. Gru'ev, "Spray Cooling of High-Temperature Metal Surfaces With High Water Pressures," *Steel in The USSR*, 1981, Vol. 11, pp. 184–186.
5. K.J. Choi and S.C. Yao, "Mechanisms of Film Boiling Heat Transfer of Normally Impacting Spray," *International Journal of Heat and Mass Transfer*, 1987, Vol. 30, pp. 311–318.
6. S.C. Yao and K.J. Choi, "Heat Transfer Experiments of Mono-Dispersed Vertically Impacting Sprays," *International Journal of Multiphase Flow*, 1987, Vol. 13, pp. 639–648.
7. S. Deb and S.C. Yao, "Analysis on Film Boiling Heat Transfer of Impacting Sprays," *International Journal of Heat Transfer*, 1989, Vol. 32, pp. 2099–2112.
8. L. Bolle and J.C. Moureau, "Spray Cooling of Hot Surfaces: A Description of the Dispersed Phase and a Parametric Study of Heat Transfer Results," *Proc. of Two Phase Flows and Heat Transfer*, 1976, Vol. 3, pp. 1327–1346.
9. B.S. Gottfried, C.J. Lee, and K.J. Bell, "The Leidenfrost Phenomenon: Film Boiling of Liquid Droplets on a Flat Plate," *International Journal of Heat and Mass Transfer*, 1966, Vol. 9, pp. 1167–1187.
10. I. Mudawar and W.S. Valentine, "Determination of the Local Quench Curve for Spray-Cooled Metallic Surfaces," *Journal of Heat Treating*, 1989, Vol. 7, pp. 107–121.
11. T.A. Deiters and I. Mudawar, "Prediction of the Temperature-Time Cooling Curves for Three-Dimensional Aluminum Products during Spray Quenching," *Journal of Heat Treating*, 1990, Vol. 8, pp. 81–91.
12. F.P. Incropera and D.P. DeWitt, *Fundamentals of Heat and Mass Transfer*, 3rd edition, Wiley, New York. 1990.

Received September 24, 1991.